

Operation with the new tungsten divertor: ASDEX Upgrade en route to an all tungsten device

R. Neu, R. Dux, A. Kallenbach, T. Eich, A. Herrmann, C. Maggi, H. Maier, H.W. Müller,
R. Pugno, T. Pütterich, I. Radivojevic, V. Rohde and the ASDEX Upgrade Team

Max-Planck-Institut für Plasmaphysik, EURATOM-Association, 85748 Garching, Germany

Introduction

Tungsten is considered as a serious candidate for plasma facing components in ITER and future fusion reactors [1]. After the successful operation with a full W divertor in 1995/1996 (W DivI) ASDEX Upgrade pursued the progressive increase of W PFCs in the main chamber since 1999 [2]. For the 2003/2004 campaign, another 10.2 m² of W coated PFCs have been added to the already existing 14.6 m². One major component, which was coated recently, is the upper divertor. Since larger erosion is expected there, 4 µm of W were deposited by plasma arc deposition at Plansee instead of 1 µm W, used previously. Now, the central column, the upper passive stabiliser loop, the complete upper divertor as well as the baffles at the lower divertor are W coated, representing about 65% of all plasma facing components. Additionally, one of the guard limiters at the low field side has been equipped with W coated tiles. Spectroscopic diagnostic has been implemented in order to quantify closely the influx from all W surfaces.

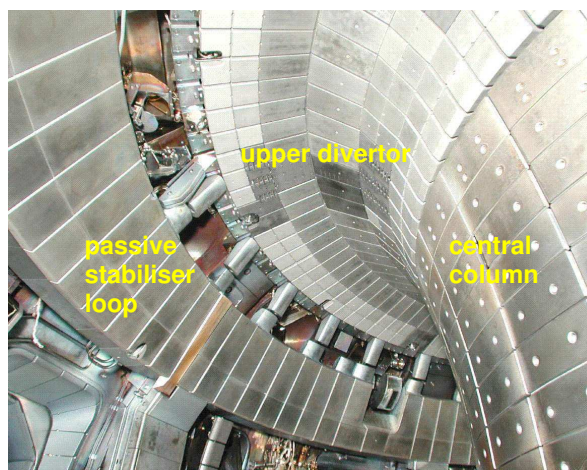


Fig. 1: View into the upper divertor of ASDEX Upgrade. The graphite tiles were coated by 4 µm of W deposited by PVD. The central column and the upper passive stabiliser loop were already coated previously by 1 µm W.

Operation with tungsten divertor and tungsten first wall

The W coatings had been previously tested in thermal screening experiments up to melting conditions [3] and by cyclic power loads, showing no failure under the specified conditions. However, during a recent vent of the machine it became evident, that a few of the newly installed W tiles exhibit delamination of the coating at the tiles edges. Since this was also observed at region with low or negligible power load, it was attributed to problems in the preparation or the production of the coating. Independently, melting of the W layer was found at the tile edges in the strike point region of the upper divertor. In contrast to the arrangement chosen for W DivI, no tilting of the strikepoint tiles was applied in order to allow for an independent choice of I_p and B_t . As a consequence, the leading edges of the tiles are exposed to a power load which may be higher by a factor of up to 10 compared to the one of the strike zone on the mean surface. None of the tiles was exchanged during the intervention, only loosely bound redeposited W surface layers were removed.

Most of the experimental programme of ASDEX Upgrade could be performed without serious limitations resulting from tungsten contamination of the main plasma and the W concentration (c_W) usually stayed below a few 10^{-5} . Unlike with carbon PFCs, a

strong difference between limiter and divertor operation is found and care has to be taken in designing the plasma shape in order to provide an adequate wall clearance [4]. In discharges with peaked density profiles in combination with low diffusive transport, the central c_W could be reduced drastically by applying up to a few MW central RF wave heating [2,5]. ELM-free discharges or discharges with low ELM frequency, as are encountered at the H-L power threshold, showed increased c_W . These could be overcome by controlling the ELM frequency through pellet injection [4].

The discharges run so far with upper single null (USN) comprise ordinary L- and H-modes as well as plasmas with internal transport barrier. Discharges with low power NBI beam heating show increased W concentrations, but in most scenarios, there is no obvious difference to discharges run in the lower (C based) divertor (LSN). Even during a continuous transition from USN to LSN no significant change in the W content could be identified. This is exemplified in Fig.2. The upper two rows of the figure show global plasma parameters together with D_α measured in the lower divertor. After a short limiter phase until $t=0.85$ s, the configuration is USN until about 3.3 s followed by a LSN phase of 1.4 s. Backtransition to USN occurs at 5.7 s, and finally, the discharge is terminated in a limiter configuration at the W coated central column for $t > 6.5$ s. The transition between USN and LSN is clearly visible in the power flowing to the corresponding divertor $P_{div,up}$ and $P_{div,dn}$. The thermo current I_{thermo}^{up-div} is measured in the upper inner divertor. It is roughly proportional to the electron temperature T_e of the divertor plasma [6]. The two lowest time traces illustrate the temporal behaviour of the tungsten density n_W and concentration c_W in the main plasma deduced from spectroscopy [7].

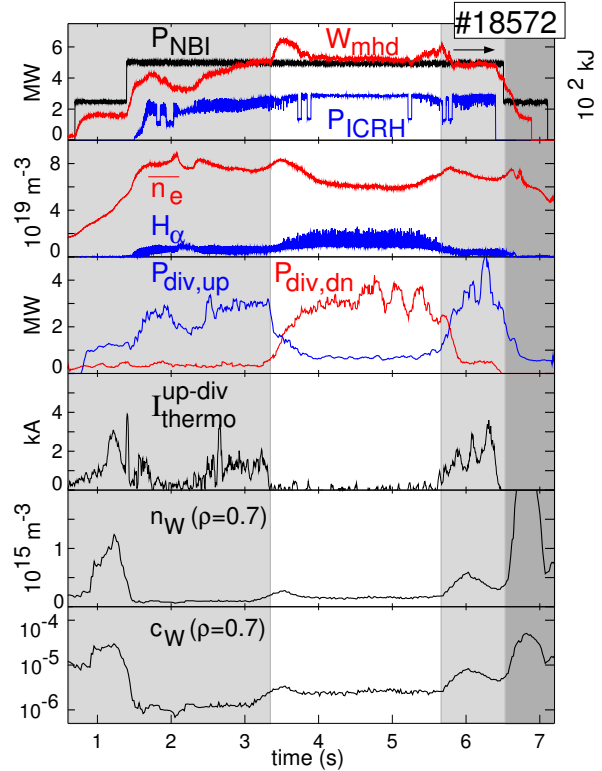


Fig. 2: Time traces for discharge #18572 with a continuous transition from USN (W coated tiles, light grey) to LSN (C tiles) and back again. During ramp down at $t > 6.5$ s, the discharge is limited at the W coated central column (dark grey).

The tungsten density n_W and concentration c_W in the main plasma deduced from spectroscopy [7]. The W-concentration is very low throughout the flat-top phase of the discharge, and n_W is very similar in both divertor phases. The increase of n_W at 1.3 s and 6.0 s may be partly attributed to higher divertor T_e , indicated by I_{thermo}^{up-div} . The change of the confinement for the different divertors can be attributed to the different H-mode thresholds for opposite $B \times \nabla B$ drift directions with respect to the X-point location, which leads to different ELM regimes as already observed with a graphite upper divertor [8]. The decrease of the background density during the LSN phase is caused by the strongly increased pumping capacity. It should be noted that the discharge, where melting on the leading edges occurred, was already performed before the above shown discharge.

Substitution of C radiation in integrated scenarios

Special emphasis is devoted to the investigation of the influence of seeded impurities on the tungsten source since a future carbon free device will crucially depend on radiative cooled scenarios in order to mitigate the divertor power load. At the same time it has to be ensured that the W source is not unduly enlarged by sputtering through the seeded impurities. Tungsten sputtering yields are shown in Fig. 3 for C, Ne, Ar and Kr multiplied by their estimated concentration in a realistic scenario. as a function of edge temperature, assuming $E_{\text{impact}} = 3ZT + 2T$. The trace impurity concentration is assumed to vary with $1/Z$, since the main plasma $\Delta P_{\text{rad}}/\Delta Z_{\text{eff}}$ rises with the impurity charge [6]. A slight reduction of the eroded W flux for typical SOL and divertor temperatures is expected when carbon is exchanged by a seed radiator with the assumed concentration. Virtually no difference is observed between Ne, Ar and Kr, taking into account the radiative efficiency rising with Z .

Experiments with argon seeding [6] resulted in a significant reduction of the power flow into the divertor. At the same time, spectroscopic measurements reveal a reduced carbon erosion in the divertor and the main chamber during the Ar seed phase. Nevertheless, the carbon density in the plasma did not drop accordingly, indicating an improvement of the core particle confinement, which is also evident from the rise of the electron density. Essential for the stable operation close to the H-L threshold was active ELM pacemaking [6,9] to avoid low-frequency type-I ELMs and a considerable fraction of central heating is used to avoid central impurity peaking.

Experiments with argon seeding [6] resulted in a significant reduction of the power flow into the divertor. At the same time, spectroscopic measurements reveal a reduced carbon erosion in the divertor and the main chamber during the Ar seed phase. Nevertheless, the carbon density in the plasma did not drop accordingly, indicating an improvement of the core particle confinement, which is also evident from the rise of the electron density. Essential for the stable operation close to the H-L threshold was active ELM pacemaking [6,9] to avoid low-frequency type-I ELMs and a considerable fraction of central heating is used to avoid central impurity peaking.

Tungsten erosion at the guard limiter

On its route to a full tungsten device, the poloidal limiters has to be transformed to a W surface. Currently, ASDEX Upgrade has 12 poloidal limiters on the low field side: a pair of side limiters for each of the 4 ICRH antennas and a pair of guard limiters at each side of the 2 neutral beam ducts, which are in between the two ICRH antenna doublets. In radial direction, the 4 guard limiters are presently about 12 mm behind the ICRH antennas. One guard limiter was equipped with 6 tungsten coated tiles. After 330 discharges, the W erosion on one tile was measured post-mortem by X-ray fluorescence analysis. Depending on the position on the tile an erosion of up to $1.2 \mu\text{m}$ was detected, which is by far the largest value found for main chamber components. At the same time no signs of melting, arcs or delamination were observed. The larger erosion at the limiter allowed for spectroscopic tungsten influx measurements [10] by monitoring the WI line radiation at 400.8 nm simultaneously with the Balmer- δ transition at 410.1 nm. The measured photon fluxes were transformed into ion fluxes using inverse photon efficiencies of $S/XB = 20$ (WI) and $S/XB = 3.3 \times 10^3$ (D_{δ} , corrected for molecular flux contribution). Since the WI line emission is more localised than the D_{δ} a correction for the spatial spread had to be applied [10].

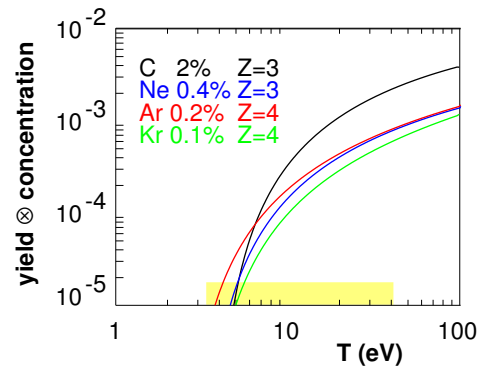


Fig. 3: Tungsten sputtering yields for different impurity species versus plasma temperature. The assumed concentrations and charge states used for the calculation are indicated in the inset.

The measured W influx densities Γ_W show a wide variation from below the detection limit ($\approx 2 \times 10^{17} \text{ m}^{-2} \text{ s}^{-1}$) in ohmically and ECR heated discharges to values of $\Gamma_W \approx 10^{19} \text{ m}^{-2} \text{ s}^{-1}$ in plasmas with ICRH or NBI heating. Transiently, even higher values of $\Gamma_W = 8 \times 10^{19} \text{ m}^{-2} \text{ s}^{-1}$ occur, when the separatrix is very close to the limiter. Γ_W exhibits a strong dependence on the distance between limiter and separatrix, with a decay length of about $\lambda = 1.5 \text{ cm}$. The quantity $Y_{eff} = \Gamma_W / \Gamma_D$ is an effective erosion yield, which includes the sputtering by deuterium as well as by plasma impurities like carbon and oxygen. It varies from below 10^{-5} to about 2×10^{-3} , and approaches 10^{-2} for transient phases. Fig. 4 shows the temporal evolution of the influxes Γ_W , Γ_D and Y_{eff} in a discharge with a continuous shift towards the low field side limiters for all five lines of sight. At the bottom the heating power from NBI and ICRH and D_α from the lower divertor is given. To interpret the yields, a knowledge of the energy spectrum of the incident ions is needed. From thermocouple measurements and Γ_D the average deposited energy per deuterium ion can be calculated for discharges with long steady state phases. It turns out that the measured Y_{eff} can only be explained by the contribution of a considerable amount ($\geq 5\%$) of fast particles from auxiliary heating [10].

Conclusions

The stepwise enhancement of the W surfaces in ASDEX Upgrade entailed a gentle increase of the average W concentration and a more demanding plasma operation. However the tools developed, enabled us to perform the whole range of aspired investigations. They allow as well to pursue the route an all W device and will be valuable for the implantation of W PFCs in future devices.

References

- [1] H. Bolt et al., J. Nucl. Mater. 307-311 (2002) 43
- [2] R. Neu et al., J. Nucl. Mater. 313 - 316 (2003) 116
- [3] H. Maier et al., Surface and Coating Technology 142-144 (2001) 733
- [4] R. Dux et al., Plasma Phys. Controlled Fusion 45 (2003) 1815
- [5] R. Neu et al., 30th EPS Conference, St. Petersburg, vol. 27A, p. P 1.123, 2003
- [6] A. Kallenbach et al., contrib. to PSI-16, Portland, 2004, submit. to J. Nucl. Mater.
- [7] T. Pütterich et al., this conference, P 4.136
- [8] A. Herrmann et al., J. Nucl. Mater. 290 - 293 (2001) 619
- [9] P.T. Lang et al., this conference, P 4.135
- [10] R. Dux et al., contrib. to PSI-16, Portland, 2004, submit. to J. Nucl. Mater.

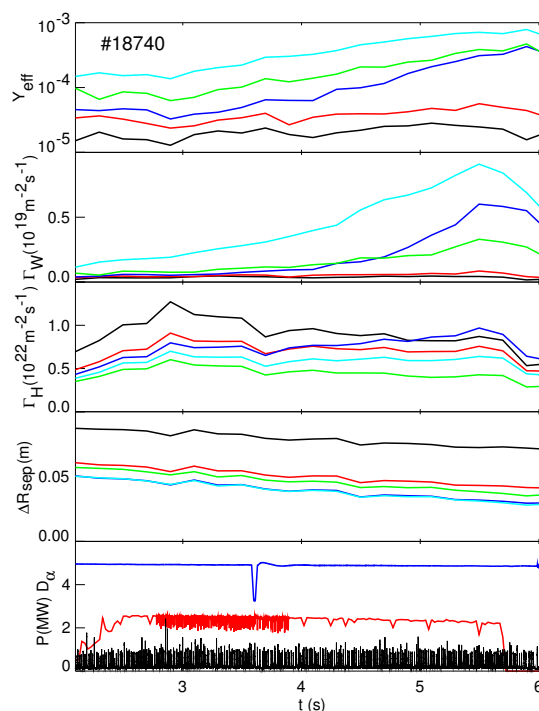


Fig. 4: Time traces for discharge #18740 with a radial shift towards the W guard limiter.